

Probing Majorana fermions in the tunneling spectra of a resonant level

R. Korytár¹ and P. Schmitteckert^{1,2}

¹Institute for Nanotechnology, Karlsruhe Institute of Technology (KIT), 76021 Karlsruhe, Germany

² DFG Center for Functional Nanostructures, Karlsruhe Institute of Technology (KIT), 76128 Karlsruhe, Germany

E-mail: richard.korytar@kit.edu

Abstract. Unambiguous identification of Majorana physics presents an outstanding problem whose solution could render topological quantum computing feasible. We develop a numerical approach to treat finite-size superconducting chains supporting Majorana fermions, which is based on iterative application of a two-site Bogoliubov transformation. We demonstrate the applicability of the method by studying a resonant level attached to the superconductor subject to external perturbations. In the topological phase, we show that the spectrum of a single resonant level allows to distinguish peak coming from Majorana physics from the Kondo resonance.

PACS numbers: 73.21.Hb, 74.55.+v, 74.78.Na

1. Introduction

Condensed matter theory, in the course of its continued quiet revolution, has endowed our understanding of nature by introducing quasi-particles with diverse, often exotic, behavior. A prominent example is a Majorana fermion[1], a particle being its own antiparticle. The possibility of synthesizing Majorana fermions has attracted a lot of attention, because of their potential for quantum computing. Information carried this way would be essentially non-local and retrieved by certain non-Abelian operations (braiding), being rather immune to general disturbances of the environment[2, 3, 4, 5]. Although several condensed matter environments could support these zero modes[6, 7, 8, 9, 10], topological superconductors [11, 12, 13] have emerged as a natural playground. The latter are not restricted to rare materials, rather they are engineered easily by forming appropriate heterostructures with ordinary s -wave superconductors[14, 15]. Experimental setups, which, based on predictions, could host Majorana fermions, have been prepared[16, 17, 18, 19], but their unambiguous experimental observation is a task far from being obvious. A very promising route is offered by transport measurements, since Majorana modes should give rise to a zero-bias resonance which does not react to weak changes of magnetic field or gate voltage.

However, conductivity enhancement near zero bias is a common companion of diverse collective phenomena. An example is Kondo effect, 0.7 anomaly [20, 21] or recently proposed electronic disorder [22]. Thus, a careful elimination of these scenarios should be a part of the “smoking - gun” probe of the Majorana particle. We would like to contribute to this debate by studying a superconducting system whose local spectral function exhibits resonances coming from two sources: the topologically protected Majorana state and a single-particle electronic resonance.

Our model system consists of a single level weakly coupled to a one-dimensional superconductor. We consider both singlet and triplet pairing mechanisms. We firstly verify, that the resonance of the single level survives after coupling to a singlet-paired superconductor. We observe that the position of the resulting resonance is coupled to the external gate voltage. When singlet pairing is replaced by the triplet one, the superconductor model is the well known Kitaev chain [12] doubled due to spin degeneracy, having Majorana states at both ends of the chain \ddagger . These modes give rise to resonances in the local spectrum at zero energy. The nature of the coupling between one of the Majorana states to the resonant level (RL) is revealed in the behavior of the resonances upon local gating and weak magnetic field. Among the plethora of peaks, the RL manifests itself due to the coupling to the external fields, in contrast to the Majorana peak. Thus, the distinctive behavior of the peak structure allows us to suggest a new means of experimental demonstration of Majorana physics.

In order to see the behavior of the resonances, it is sufficient to look at local spectral functions, which directly convey the electron/hole tunneling spectral density.

The calculation of spectra involves solving for the eigenstates of the Hamiltonian with mean-field superconducting fluctuations, i.e. a general Hermitian operator which is bilinear in fermionic operators. We employ a numerical diagonalization method based on iterative application of Bogoliubov transformation [23] to a Fock subspace spanned by two orbitals. This is an extension of the Jacobi diagonalization procedure: not only we consider basis change, but also general automorphisms of the Fermi

\ddagger Per spin, there is a single fermionic boundary mode, which corresponds to two separate Majorana states

operator algebra.

From a theoretical standpoint, this approach relies on a fully fermionic language. Thus, it is capable at providing intuitively transparent arguments, like occupation numbers, in contrast to an alternative approach, based on Majorana representation of the Hamiltonian [24]. From the experimental point, results of our work suggest a means to identify the character of close-to zero-bias resonances, and distinguish them from peaks originating from different sources, such as the charge and spin resonances of the low-temperature Anderson model.

Our paper is structured as follows: in the next section we introduce the model Hamiltonian and the diagonalization procedure. The two-orbital “dimer” not only serves as an illustration of the method, but presents a single iteration step when large chains are treated. At the end of section 2 we detail on the calculation of the local spectral function. In the Results section, we show the spectra calculated for a RL coupled to a singlet-paired and triplet-paired superconductor, contrast the differences and understand the trends of the peaks. At the end of this work, we discuss the experimental relevance of our calculations and summarize.

2. Model and methods

2.1. Hamiltonian

We study a resonant level (RL) coupled to a one dimensional spin-full superconducting chain. The Hamiltonian of the full system reads

$$\begin{aligned}
 H = & \epsilon_{0\sigma} \hat{c}_{0\sigma}^\dagger \hat{c}_{0\sigma} + t_0 \left(\hat{c}_{0\sigma}^\dagger \hat{c}_{1\sigma} + \text{h.c.} \right) \\
 & - \mu_\sigma \sum_{i=1}^N \hat{c}_{i\sigma}^\dagger \hat{c}_{i\sigma} - t \sum_{i=1}^{N-1} \left(\hat{c}_{i+1\sigma}^\dagger \hat{c}_{i\sigma} + \text{h.c.} \right) \\
 & + \Delta_S \sum_{i=1}^N \left(\hat{c}_{i\uparrow}^\dagger \hat{c}_{i\downarrow}^\dagger + \text{h.c.} \right) + \Delta_T \sum_{i=1}^{N-1} \left(\hat{c}_{i+1\sigma}^\dagger \hat{c}_{i\sigma}^\dagger + \text{h.c.} \right), \quad (1)
 \end{aligned}$$

where \hat{c}_i (\hat{c}_i^\dagger) are fermionic annihilation (creation) operators at site i . The orbital labeled 0 is the RL coupled weakly to the rest of the chain, which spans the sites 1, ..., N . The first and second term are RL’s on-site energy and hopping energy to the chain, respectively. The second line contains the chemical potential μ_σ of the chain (spin-dependence masks a Zeeman field) and the hopping term between nearest neighbour pairs of the chain. The last two terms describe superconducting pairing in the mean-field fashion: the singlet pairing with strength Δ_S and triplet pairing proportional to Δ_T . Spin index σ , wherever appears in (1), implies summation.

2.2. Diagonalization

We solve for the eigen-energies and eigenvectors of the Hamiltonian (1) numerically. Before we explain the full procedure, we illustrate few important points in the two-orbital case.

2.2.1. Dimer We start with a simple two-orbital (dimer) Hamiltonian described by

$$H = \epsilon \hat{c}_1^\dagger \hat{c}_1 + \epsilon' \hat{c}_2^\dagger \hat{c}_2 + t \left(\hat{c}_2^\dagger \hat{c}_1 + \hat{c}_1^\dagger \hat{c}_2 \right) + \Delta \left(\hat{c}_2 \hat{c}_1 + \hat{c}_1^\dagger \hat{c}_2^\dagger \right) \quad (2)$$

with two un-equal on-site terms, a hopping term and the last term describes superconducting pairing. For convenience, the Hamiltonian is written in a matrix form

$$H = \begin{pmatrix} \hat{c}_1^\dagger & \hat{c}_2^\dagger & \hat{c}_1 & \hat{c}_2 \end{pmatrix} \begin{pmatrix} \epsilon & t & 0 & \frac{\Delta}{2} \\ t & \epsilon' & -\frac{\Delta}{2} & 0 \\ 0 & -\frac{\Delta}{2} & 0 & 0 \\ \frac{\Delta}{2} & 0 & 0 & 0 \end{pmatrix} \begin{pmatrix} \hat{c}_1 \\ \hat{c}_2 \\ \hat{c}_1^\dagger \\ \hat{c}_2^\dagger \end{pmatrix}. \quad (3)$$

where the row and column vectors are similar to Nambu spinors, see Appendix C. We bring it to a diagonal form in a two-step procedure. Firstly, we transform away the anomalous pairing terms by a Bogoliubov transformation. Then the Hamiltonian attains a coupled two-level structure which can be brought to a diagonal form by a standard unitary transformation (ie a change of basis).

We wish to subject the fermion operators to a linear transformation

$$\begin{pmatrix} \hat{d}_1 \\ \hat{d}_2 \\ \hat{d}_1^\dagger \\ \hat{d}_2^\dagger \end{pmatrix} = \mathcal{U} \begin{pmatrix} \hat{c}_1 \\ \hat{c}_2 \\ \hat{c}_1^\dagger \\ \hat{c}_2^\dagger \end{pmatrix} \quad (4)$$

and ensure that the new operators $\{\hat{d}_i, \hat{d}_i^\dagger\}$ obey anti-commutation relations. It follows that the 4×4 matrix \mathcal{U} must be unitary. We write it in the block form

$$\mathcal{U} = \begin{pmatrix} U & V \\ V' & U' \end{pmatrix} \quad (5)$$

with each sub-matrix U, U', V, V' containing 2×2 elements, so that $\hat{d}_i = U_{ij}\hat{c}_j + V_{ij}\hat{c}_j^\dagger$ and $\hat{d}_i^\dagger = V'_{ij}\hat{c}_j + U'_{ij}\hat{c}_j^\dagger$ (Einstein summation). It follows that $U' = U^*$ and $V' = V^*$ and the transformation matrix must have the following structure

$$\mathcal{U} = \begin{pmatrix} U & V \\ V^* & U^* \end{pmatrix}. \quad (6)$$

Unitarity implies

$$\begin{aligned} UU^\dagger + VV^\dagger &= 1 \\ UV^\top + VU^\top &= 0, \end{aligned} \quad (7)$$

with V^\top (U^\top) the transposed of V (U). We detail in Appendix on how to choose U and V so that the transformed Hamiltonian is free from anomalous terms of the form $d_1 d_2$.

Then, the Hamiltonian can be rearranged to a normal-ordered form

$$H = \Psi^\dagger \begin{pmatrix} \epsilon'_1 & t' & 0 & 0 \\ t' & \epsilon'_2 & 0 & 0 \\ 0 & 0 & 0 & 0 \\ 0 & 0 & 0 & 0 \end{pmatrix} \Psi \quad (8)$$

where we introduced $\Psi^\dagger = (\hat{d}_1^\dagger \hat{d}_2^\dagger d_1 d_2)$. We achieve the diagonalization by the transformation of the kind (4) with the structure of the unitary matrix

$$\mathcal{U}'' = \begin{pmatrix} U'' & 0 \\ 0 & U'' \end{pmatrix}. \quad (9)$$

This is, of course, a standard eigenvalue problem of a two-level system.

2.2.2. Chain Our numerical diagonalization of the full Hamiltonian consists of iterative application of the procedure shown in the preceeding section. Firstly, one singles out two orbitals in the Hilbert space, then applies the Bogoliubov transformation that removes pairing of the selected “dimer”, then transforms the remaining parts of the Hamiltonian accordingly.

Here we detail on the outlined procedure. Let us consider a general Hamiltonian of a Bogoliubov-de Gennes type

$$H = \mathbf{\Gamma}^\dagger \mathcal{H} \mathbf{\Gamma} \quad (10)$$

where $\mathbf{\Gamma}^\dagger := (c_1^\dagger, \dots, c_N^\dagger, c_1, \dots, c_N)$ is a row vector of fermion operators labeled by indices of an orthonormal basis set (spin and orbital) and \mathcal{H} is a $2N \times 2N$ matrix. The assignment of the matrix elements of \mathcal{H} is ambiguous and in what follows we will require the following $N \times N$ block structure

$$\mathcal{H} = \begin{pmatrix} h & b \\ -b & 0 \end{pmatrix} \quad (11)$$

with $h^\dagger = h$ and $b^\dagger = -b$. The fermionic operator algebra allows for linear automorphisms $\mathbf{\Gamma}' = \mathcal{U} \mathbf{\Gamma}$ by the means of a unitary matrix \mathcal{U} with the $N \times N$ block structure

$$\mathcal{U} = \begin{pmatrix} U & V \\ V^* & U^* \end{pmatrix}. \quad (12)$$

We wish to find a matrix \mathcal{U} , which carries away all pairing and hopping terms from the Hamiltonian. In addition we demand that the transformed operators still obey fermionic anti-commutations relations which again leads to the condition (7). It is important to note that this implies \mathcal{U} being unitary. However, an arbitrary unitary \mathcal{U} matrix will in general not adhere to the form (12) and therefore not conserve the fermionic anti-commutation relations. Therefore, just diagonalizing matrix \mathcal{H} will in general not lead to a valid solution. One may argue that any unitary matrix that diagonalizes \mathcal{H} should lead to the same solution. However, this does not apply here. The transformation we describe below will in general not lead to a completely diagonal matrix. Instead it will transform the matrix into a form where the off-diagonal symmetric part of h and the asymmetric part of b vanishes. In addition the ‘0’ in (11) may not be zero. Therefore, the resulting matrix only leads to a Hamiltonian that is equivalent to a diagonal form for fermionic operators.

In order to ensure the structure (12) we developed an iterative procedure, sketched in the following steps (i-iii). Suppose that at the p ’th step we were given a matrix \mathcal{H}_p – of the form (11).

- (i) We identify a pair of orbitals with the largest pairing, say $m < n \leq N$. The operator set $c_m, c_n, c_m^\dagger, c_n^\dagger$ is transformed to a new operator set $c'_m, c'_n, c'^{\dagger}_m, c'^{\dagger}_n$, $m < n \leq N$ in which the pairing vanishes. This amounts to solving the “dimer” problem from the previous section.
- (ii) The matrix \mathcal{H}_p becomes $\mathcal{H}_{p+1} = \mathcal{U}_p \mathcal{H}_p \mathcal{U}_p^\dagger$ when expressed in the new operator set, the matrix \mathcal{U}_p does not mix operators with index other than m or n ; in the dimer Fock subspace has the structure as in equations (7,6).
- (iii) The Hermitian matrix \mathcal{H}_{p+1} is to be brought to a form (11) by a permutation of fermionic operators. Note, that this step eventually generates a c -number term to the Hamiltonian which can be discarded.

After all pairings are lower than a certain tolerance, we perform a basis change to rotate away hoppings. This can be achieved by the transformation matrix (12) with zero off-diagonal blocks and is a routine task. All results presented in this work were calculated by this iterative method; the Hamiltonian was thought converged if the absolute value of the highest pairing was smaller than $10^{-10}t$. We collect the product of all transformation matrices in order to calculate local quantities.

2.3. Spectral function

Let the Hamiltonian (1) be transformed to a diagonal form

$$H = \sum_i E_i \hat{d}_i^\dagger \hat{d}_i$$

by $d_i = \sum (U_{ij} \hat{c}_j + V_{ij} \hat{c}_j^\dagger)$.

The normal-component retarded Green's function at site i reads

$$G_{ii}(\omega) = \langle | \hat{c}_i \frac{1}{\omega - H + i\eta} \hat{c}_i^\dagger + \hat{c}_i^\dagger \frac{1}{\omega + H + i\eta} \hat{c}_i | \rangle.$$

The spectral function is given by the expression

$$A_{ii}(\omega) = -\frac{1}{\pi} \Im \sum_j \left[\frac{|U_{ij}|^2}{\omega - E_j + i\eta} + \frac{|V_{ij}|^2}{\omega + E_j + i\eta} \right] \quad (13)$$

where η is a positive infinitesimal, which in the numerics will be substituted by a finite value of the order of the average level splitting around the Fermi level in the absence of superconductivity. Hereafter we shall use $\eta = 0.015t$. The resulting spectra are deconvoluted by the algorithm of the reference [25] (poor man's deconvolution).

3. Results

From now on, all numerical values of dimension energy (such as pairings, on-site energies, *etc.*) will be in the units of t .

The Hamiltonian (1) is studied in two regimes:

- (i) a resonant level coupled to a singlet-paired superconductor ($\Delta_T = 0, \Delta_S = 0.6$)
- (ii) a resonant level coupled to a triplet-paired superconductor ($\Delta_S = 0, \Delta_T = 0.3$)

Thus, the superconducting bulk gap will be 2.4 in both cases. The rest of the chain Hamiltonian is parameterized as $\mu = 0$ and $t = 1$ as the unit of energy. In all cases, the superconducting chain has 200 sites. The RL is weakly coupled to the chain with $t_0 = 0.3$ and on-site energy $\epsilon_{0\sigma}$ will vary.

Hence, the case (ii) is in a topologically non-trivial phase [12] with Majorana modes. The first case is a topologically trivial superconducting state.

3.1. Behavior of local spectral function on gating

In figure 1 we show several spectral function for case (i). There are no zero-modes. The position of the highest peak coincides with the on-site energy of the resonant level ϵ_0 . Along with this RL peak, there is an Andreev-reflected peak roughly at $-\epsilon_0$. The mirroring behavior of the resonant and Andreev peak positions as the "gate" varies is a known distinctive feature of the Andreev process. Finally, in the outside region

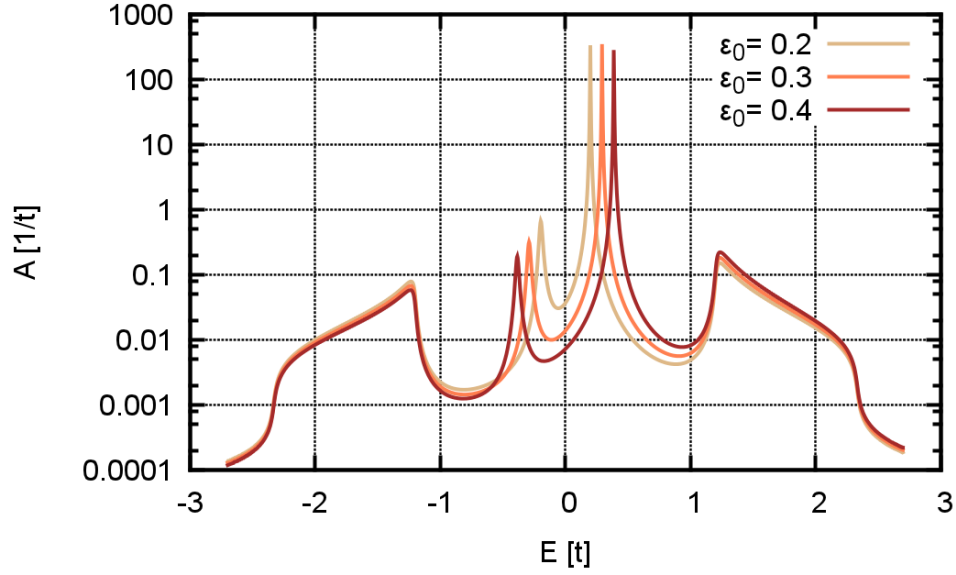


Figure 1. Spectral function of a resonant level coupled to a singlet-paired superconductor chain with 200 sites. The resonant level couples via hopping $t_0 = 0.3$ to the chain. Three curves correspond to different on-site energies of the level.

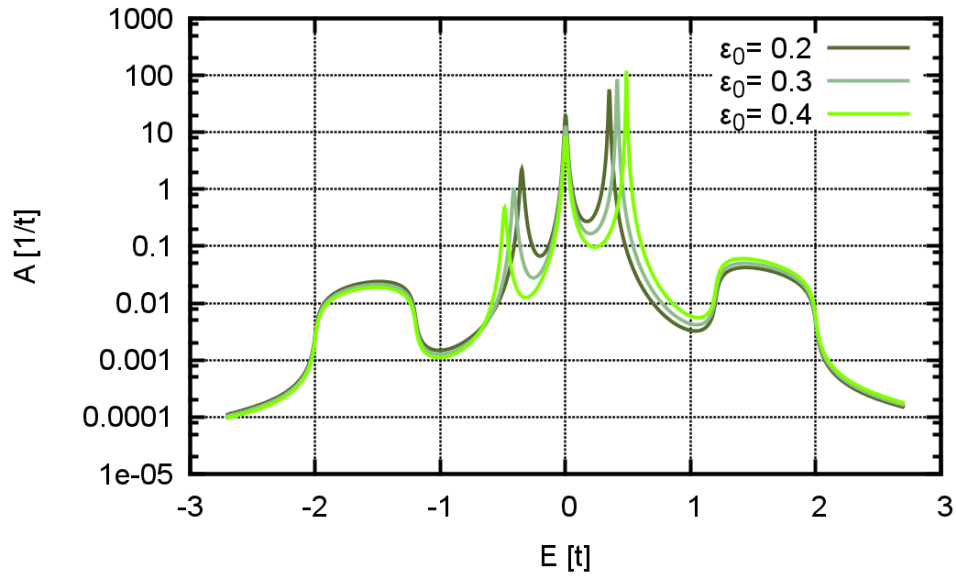


Figure 2. Spectral function of a resonant level coupled to a triplet-paired superconductor chain with 200 sites. The resonant level couples via hopping $t_0 = 0.3$ to the chain. Three curves correspond to different on-site energies of the level.

$|E| > t$ two ridge-like features appear. These are the bulk features of an ordinary superconductor.

Now we proceed to the case (ii), the topological superconductor, figure 2. A strikingly new feature is the zero-energy peak, which signals the spreading of the Majorana mode to the RL site. Note that the position of the RL is repelled from the bare value, the resonance center is shifted upwards. This can be understood as a delocalization of the Majorana fermion: without the resonant state, the Hamiltonian in regime (ii) reduces to a spin-full Kitaev chain with zero modes localized at both edges. Coupling to the RL dilutes the Majorana state [26]; however, since its energy is fixed to zero, the coupling-induced splitting can affect the RL position only.

3.2. Magnetic field dependence of local spectral function

After seeing the distinct behavior of peaks under gating, we proceed to study the dependence of spectra in a weak magnetic field applied to the whole system. We introduce a homogeneous Zeeman field by substituting $\epsilon_{0\sigma} = \epsilon_0 + \sigma B/2$ and $\mu_\sigma = \mu + \sigma B/2$, $\sigma = \pm 1$ in the Hamiltonian (1). Hence, B is the spin splitting of a single level.

In the singlet paired case the RL and its Andreev reflected counterpart split, as shown in figure (3). Note that in the highest splitting $B = 2t_0$ an *accidental* zero-energy resonance forms from the overlap of two resonances. The magnitude of peak splitting obeys strictly the Zeeman term in the RL Hamiltonian.

As the last case, we treat the influence of Zeeman field on the triplet-paired superconductor, case (ii)§. The pinning of the Majorana state to the zero energy (the chemical potential) is robust against weak magnetic field, too. The magnetic field, however, splits the resonant and Andreev levels. Figure (4) shows evolution of the spectral function for the Zeeman fields $B = 0, t_0$ and $2t_0$. The side peaks are clearly split while the central resonance stays almost intact. Again, all peaks “interact” and apart from the previously mentioned shift of the Andreev and resonant levels off the zero energy, there is also a decrease in the spin splitting below the value given by B .

4. Discussion

As stated in the introduction, zero bias transport features can arise in solid-state systems due to reasons unrelated to Majorana physics.

A thoroughly studied example is Kondo effect. In the transport through quantum wires, Kondo physics could emerge due to enhancement of Coulomb interactions (due to reduced screening) or presence of a magnetic impurity in the wire. The spectral manifestation at low temperatures is the zero-energy Kondo resonance (width of the order of the Kondo temperature $k_B T_K$) and possibly charge peaks of the Anderson model. The side peaks need not be symmetric around the Fermi level and behave differently when external fields are introduced. A change of the gate voltage (on-site energy of the Anderson impurity) causes the lower and higher side peaks move *in the same sense*, accompanied by a pronounced change in the width of the central (Kondo) resonance. This is in sharp contrast with the case of a RL coupled to a Majorana fermion (compare to figure 2), where side peaks move off the zero bias symmetrically and the central resonance stays intact.

§ We remark that this part applies to the realizations of topological superconductivity where spin degeneracy remains.

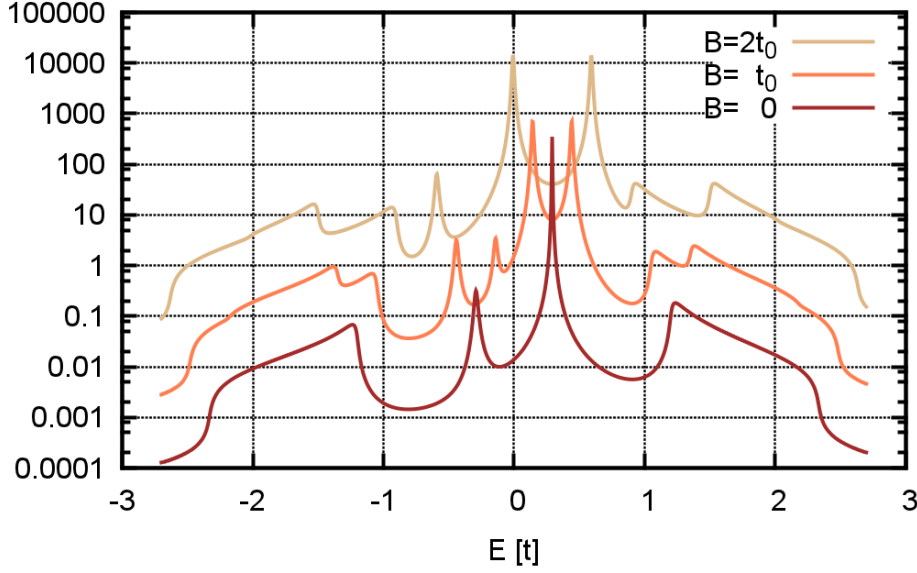


Figure 3. Spectral function of a resonant level weakly coupled to a singlet-paired superconductor with 200 sites. The three curves represent different values of a homogeneous Zeeman field, each curve is a sum over two projections of spin. B denotes the splitting of a single level and is expressed in multiples of the resonant level hopping t_0 . For clarity, the spectra have been shifted vertically.

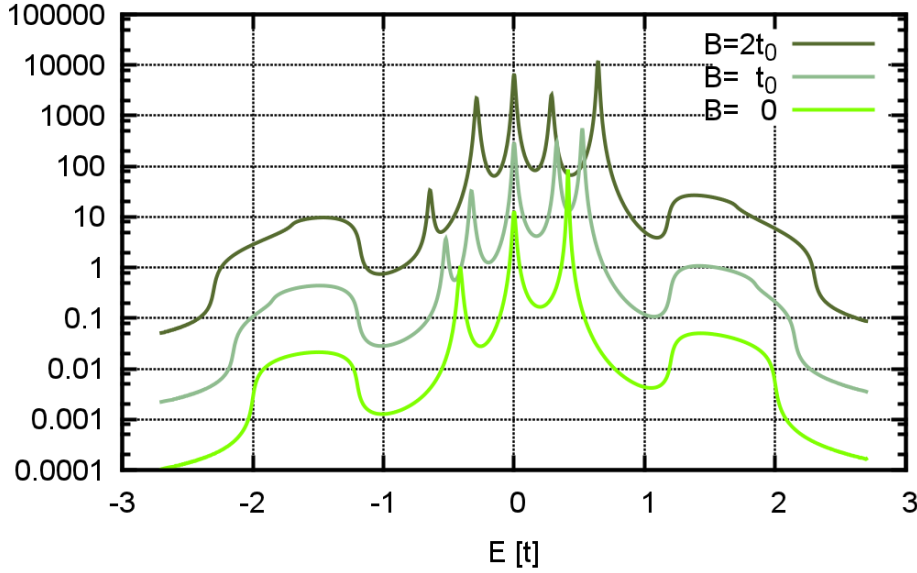


Figure 4. Spectral function of a resonant level weakly coupled to a triplet-paired superconductor with 200 sites. The three curves represent different values of a homogeneous Zeeman field, each curve is a sum over two projections of spin. B denotes the splitting of a single level and is expressed in multiples of the resonant level hopping t_0 . For clarity, the spectra have been shifted vertically.

Further distinction emerges when studying the Zeeman splitting. Majorana resonance does not split even though the side peaks do (figure 4). The Kondo resonance, in contrary, is immune only for weak fields and splits when the Zeeman field becomes of the order of $k_B T_K$, ie of the order of the peak width. The resulting splitting of the zero energy peak is then twice the Zeeman splitting. Hence, magnetic field and local gating are both independently sufficient to distinguish between both underlying mechanisms.

5. Conclusions

We have developed an efficient numerical approach capable to treat hybrid inhomogeneous systems. Our method relies on a fully fermionic formalism, that is, eigenstates of the Hamiltonian are fermions. We diagonalize the Hamiltonian by the means of a unitary matrix and point out that the matrix structure must be restricted in order to satisfy anti-commutation algebra.

We have applied the method to the combined system of a resonant level (RL) and a superconducting chain. Regardless of the nature of pairing, gate voltage and magnetic fields couple to the RL, as we show in the analysis of the level's spectral function. When triplet pairing is introduced, the local spectral function attains a zero-bias resonance, which does not react to external fields. In summary, the combined system allows to prove that the perturbing field does couple to the system, at the same time demonstrating the presence of a Majorana mode.

Apart from a direct access to spectral functions, the fermionic language could be conveniently used to calculate other local quantities, as for instance wave functions of the zero modes. Alicea *et al.* [4] have elaborated on the possibility to implement quantum memory in a network of topological superconducting wires. Here, the braiding operation could be realized by changes in local gate voltages. Our method, straightforwardly extended to non-stationary regimes, offers a way to simulate braiding while tracking the Majorana state in real time.

Acknowledgments

PS would like to thank Stephan Rachel, Pascal Simon, Ronny Thomale, and Johannes Reuther for stimulating discussions.

Appendix A. Single angle Bogoliubov transformation

In section 2.2.1 we introduced general conditions for the transformation matrix of the dimer fermion operators. In order to rotate the Hamiltonian in a particle conserving representation we have to rotate the asymmetric part of B to zero. In recipe described above we have reduced the problem to solving a two site system which can be achieved via a standard fermionic Bogoliubov transformation

$$\hat{d}_1 = \cos(\beta)\hat{c}_1 - \sin(\beta)\hat{c}_2^+ \quad (\text{A.1})$$

$$\hat{d}_2 = \cos(\beta)\hat{c}_2 + \sin(\beta)\hat{c}_1^+, \quad (\text{A.2})$$

which fulfill the conditions (7). In matrix form they are given by

$$U = \begin{pmatrix} \cos(\beta) & 0 \\ 0 & \cos(\beta) \end{pmatrix} \quad V = \begin{pmatrix} 0 & -\sin(\beta) \\ \sin(\beta) & 0 \end{pmatrix}. \quad (\text{A.3})$$

Using

$$\tan(2\beta) = -\frac{2\Delta}{\epsilon + \epsilon'}. \quad (\text{A.4})$$

the Δ contribution to Hamiltonian H in (2) is transformed to zero.

Appendix B. Two angle Bogoliubov transformation

In addition to transforming the Δ part to zero, we can also rotate the t contribution to zero by applying an additional rotation

$$R = \begin{pmatrix} \cos(\alpha) & -\sin(\alpha) \\ \sin(\alpha) & \cos(\alpha) \end{pmatrix} \quad U_R = R \cdot U \quad V_R = R \cdot V, \quad (\text{B.1})$$

where the rotation angle is given by

$$\tan(2\alpha) = -\frac{2t}{\epsilon - \epsilon'}. \quad (\text{B.2})$$

Appendix C. Remarks on Nambu spinors

In the case of s -wave pairing one usually resorts to Nambu spinors

$$\Psi_x^\dagger = \begin{pmatrix} \hat{c}_{x,\uparrow}^\dagger & \hat{c}_{x,\downarrow}^\dagger & \hat{c}_{x,\downarrow} & -\hat{c}_{x,\uparrow} \end{pmatrix}. \quad (\text{C.1})$$

Using the label $j = 2x$ for the up spins and $j = 2x + 1$ to the down spins this corresponds to a matrix representation using a transformation of the form

$$\mathcal{U}_N = \begin{pmatrix} 1 & 0 \\ 0 & U_N \end{pmatrix}, \quad (\text{C.2})$$

where U_N block diagonal consisting of 2×2 rotation matrices with an angle of $\pi/2$. Using this transformation one is led to a matrix where the new \tilde{b} block is actually symmetric. The disadvantage of the Nambu representation is that the conditions for preserving canonical anti-commutation relations are not as simple as eq. (7) in our representation.

Appendix D. Remarks on the numerics

For the recipe of bringing the many site problem to diagonal form it is sufficient to use the single angle version. In our tests it turned out that the two angle version actually needs less iteration step to converge. However, each step costs approximately twice as the number of vector operations is doubled. In return the single angle version was typically faster.

One can also start the procedure by first rotating b into a tridiagonal form using the algorithm of [24]. Moreover, an anti-symmetric matrix can be transformed into a 2×2 -block diagonal matrix $D = Q \cdot b \cdot Q^\dagger$ with Q unitary [27, 28]. Since D consists only of 2×2 and 1×1 blocks with a diagonal of zeroes D^2 is diagonal. Therefore we have

$$D^2 = Q \cdot b \cdot Q^\dagger \cdot Q \cdot b \cdot Q^\dagger = Q \cdot b^2 \cdot Q^\dagger, \quad (\text{D.1})$$

where Q is given by the diagonalization of b^2 . Note, that it is essential that b is used in the antisymmetric form $b = -b^\top$. Starting our procedure with $U = Q$ and $V = 0$ leads to an initial 2×2 -block diagonal matrix b leading to an improved convergence rate in our tests.

- [1] Ettore Majorana. Teoria simmetrica dell'elettrone e del positrone. *Il Nuovo Cimento*, 5:171–184, 1937.
- [2] Frank Wilczek. Majorana returns. *Nature Physics*, 5(9):614–618, 2009.
- [3] C.W.J. Beenakker. Search for majorana fermions in superconductors. *Annual Review of Condensed Matter Physics*, 4(1):113–136, 2013.
- [4] Jason Alicea, Yuval Oreg, Gil Refael, Felix von Oppen, and Matthew PA Fisher. Non-abelian statistics and topological quantum information processing in 1d wire networks. *Nature Physics*, 7(5):412–417, 2011.
- [5] Jason Alicea. New directions in the pursuit of majorana fermions in solid state systems. *Reports on Progress in Physics*, 75(7):076501, 2012.
- [6] Liang Jiang, Takuya Kitagawa, Jason Alicea, A. R. Akhmerov, David Pekker, Gil Refael, J. Ignacio Cirac, Eugene Demler, Mikhail D. Lukin, and Peter Zoller. Majorana fermions in equilibrium and in driven cold-atom quantum wires. *Phys. Rev. Lett.*, 106:220402, Jun 2011.
- [7] N. Read and Dmitry Green. Paired states of fermions in two dimensions with breaking of parity and time-reversal symmetries and the fractional quantum hall effect. *Phys. Rev. B*, 61:10267–10297, Apr 2000.
- [8] Xiao-Liang Qi, Taylor L. Hughes, and Shou-Cheng Zhang. Chiral topological superconductor from the quantum hall state. *Phys. Rev. B*, 82:184516, Nov 2010.
- [9] D. A. Ivanov. Non-abelian statistics of half-quantum vortices in p -wave superconductors. *Phys. Rev. Lett.*, 86:268–271, Jan 2001.
- [10] Ronny Thomale, Stephan Rachel, and Peter Schmitteckert. Tunneling spectra simulation of interacting majorana wires. *arXiv:1306.5127*, (unpublished).
- [11] Liang Fu and C. L. Kane. Superconducting proximity effect and majorana fermions at the surface of a topological insulator. *Phys. Rev. Lett.*, 100:096407, Mar 2008.
- [12] A Yu Kitaev. Unpaired majorana fermions in quantum wires. *Physics-Uspekhi*, 44(10S):131, 2001.
- [13] Martin Leijnse and Karsten Flensberg. Introduction to topological superconductivity and majorana fermions. *Semiconductor Science and Technology*, 27(12):124003, 2012.
- [14] Roman M. Lutchyn, Jay D. Sau, and S. Das Sarma. Majorana fermions and a topological phase transition in semiconductor-superconductor heterostructures. *Phys. Rev. Lett.*, 105:077001, Aug 2010.
- [15] Yuval Oreg, Gil Refael, and Felix von Oppen. Helical liquids and majorana bound states in quantum wires. *Phys. Rev. Lett.*, 105:177002, Oct 2010.
- [16] V. Mourik, K. Zuo, S. M. Frolov, S. R. Plissard, E. P. A. M. Bakkers, and L. P. Kouwenhoven. Signatures of majorana fermions in hybrid superconductor-semiconductor nanowire devices. *Science*, 336(6084):1003–1007, 2012.
- [17] Anindya Das, Yuval Ronen, Yonatan Most, Yuval Oreg, Moty Heiblum, and Hadas Shtrikman. Zero-bias peaks and splitting in an al-inas nanowire topological superconductor as a signature of majorana fermions. *Nature Physics*, 8(12):887–895, 2012.
- [18] Leonid P Rokhinson, Xinyu Liu, and Jacek K Furdyna. The fractional ac josephson effect in a semiconductor-superconductor nanowire as a signature of majorana particles. *Nature Physics*, 8(11):795–799, 2012.
- [19] M. T. Deng, C. L. Yu, G. Y. Huang, M. Larsson, P. Caroff, and H. Q. Xu. Anomalous zero-bias conductance peak in a nbinsb nanowirenb hybrid device. *Nano Letters*, 12(12):6414–6419, 2012.
- [20] S. M. Cronenwett, H. J. Lynch, D. Goldhaber-Gordon, L. P. Kouwenhoven, C. M. Marcus, K. Hirose, N. S. Wingreen, and V. Umansky. Low-temperature fate of the 0.7 structure in a point contact: A kondo-like correlated state in an open system. *Phys. Rev. Lett.*, 88:226805, May 2002.
- [21] L. P. Rokhinson, L. J. Guo, S. Y. Chou, and D. C. Tsui. Kondo-like zero-bias anomaly in electronic transport through an ultrasmall si quantum dot. *Phys. Rev. B*, 60:R16319–R16321, Dec 1999.
- [22] Dmitry Bagrets and Alexander Altland. Class d spectral peak in majorana quantum wires. *Phys. Rev. Lett.*, 109:227005, Nov 2012.
- [23] NN Bogoliubov. On the theory of superfluidity. *J. Phys.(USSR)*, 11(23):4–2, 1947.
- [24] M Wimmer. Algorithm 923: Efficient numerical computation of the pfaffian for dense and banded skew-symmetric matrices. *ACM Transactions on Mathematical Software (TOMS)*, 38(4):30, 2012.
- [25] Peter Schmitteckert. Calculating green functions from finite systems. In *Journal of Physics: Conference Series*, volume 220, page 012022. IOP Publishing, 2010.
- [26] Marco Gibertini, Fabio Taddei, Marco Polini, and Rosario Fazio. Local density of states in

- metal-topological superconductor hybrid systems. *Phys. Rev. B*, 85:144525, Apr 2012.
- [27] R. C. Ward and L. J. Gray. Eigensystem computation for skew-symmetric and a class of symmetric matrices. *ACM Trans. Math. Softw.*, 4(3):278–285, September 1978.
- [28] Gene H. Golub and Charles F. Van Loan. *Matrix computations (3rd ed.)*. Johns Hopkins University Press, Baltimore, MD, USA, 1996.